Hindawi
Journal of Nanomaterials
Volume 2019, Article ID 9457683, 10 pages
https://doi.org/10.1155/2019/9457683

Research Article

Interactions of Carbon Nanotubes and Carbon Nanohorns with a Model Membrane Layer and Lung Surfactant In Vitro

Dorota Kondej[1] **and Tomasz R. Sosnowski**[2]

[1]*Central Institute for Labour Protection-National Research Institute, Czerniakowska 16, Warsaw, Poland*
[2]*Faculty of Chemical and Process Engineering, Warsaw University of Technology, Waryńskiego 1, 00-645 Warsaw, Poland*

Correspondence should be addressed to Tomasz R. Sosnowski; Tomasz.Sosnowski@pw.edu.pl

Received 31 August 2018; Accepted 25 November 2018; Published 10 February 2019

Academic Editor: Enrico Bergamaschi

A broader use of carbon nanomaterials increases the risk of their inhalation as aerosol dispersed in the air. Inhaled nanometer-sized particles are known to penetrate to the pulmonary region where they interact with the lung surfactant as the first barrier they meet and eventually penetrate to the surface of the cellular layer. This study presents the results of experimental studies of physicochemical interactions between several types of carbon nanomaterials (nanotubes and nanohorns of various size and surface properties) and lipid layers in two qualitatively different experimental systems: Langmuir trough and pulsated drop tensiometer, both providing complementary possibilities to study interfacial properties of the lipid-rich layer. Quantified alterations in mechanical properties if lipid films (equilibrium compressibility, dynamic surface elasticity, and viscosity) indicate that nanocarbons with different wettability may induce concentration-dependent frustration of the lung surfactant and biological membranes in vivo. The observed effects are discussed not only in relation to health effects from nanoparticle inhalation but also to potential medical applications of engineered carbon nanomaterials.

1. Introduction

The respiratory system is a primary gate for nanoparticle (NP) entrance to the organism [1, 2], which is facilitated by the fact that NPs are very light, easily aerosolized, and remain suspended in the air for a long time. In the era of many new manmade nanomaterials, the hazard of their accidental inhalation increases. An important group of such materials is carbon nanomaterials (CNMs) including carbon nanotubes (CNTs) and nanohorns (CNHs) with different size and structure (e.g., single-walled: SWCNTs or multiwalled: MWCNTs). It is estimated than CNTs constitute almost 30% value of the total market of nanomaterials [3]. A large evidence exists regarding the influence of CNTs on the respiratory system [4–6]. The concentration of CNTs in industrial and research facilities may be in the order of hundreds $\mu g/m^3$ [7] which leads to substantial load of deposited nanomaterials in the pulmonary system. Health effects of inhaled CNTs depend on their size, architecture, and surface properties. The latter can be modified by functionalization of carbon nanomaterials which is often done to obtain a desired wettability and reactivity in their further practical applications [8].

NP size and shape determines the region of particle deposition in the lungs and the bioavailability which increases as particle size is reduced [9]. NPs with size of 10-100 nm are known to penetrate and deposit in the alveolar region of the respiratory system with the efficiency of 20-60% [10]. Retention time of carbon nanomaterials in the lungs is above 48 h [6, 11] which facilitates their penetration to the epithelial cells, blood, and lymph [12, 13]. Such nanomaterials can be dislocated through the biological membranes and migrate to various organs [9], including the brain [14]. On the other hand, carbon nanomaterials are proposed as candidates for diagnostic particles and drug carriers [15], which usually requires their physicochemical functionalization [16]. These potential applications indicate the need of the thorough analysis of the influence of carbon nanomaterials characterized by variable surface properties, on the biological membranes. DPPC monolayer is often considered the simplest functional model of such membranes both in

Table 1: Physical data of carbon nanomaterials used in the studies.

CNM designation in this study	Nanomaterial description and the supplier	External particle diameter (nm)	Internal particle diameter (nm)	Length (nm)	SSA* (m^2/g)
I	Multiwalled carbon nanotubes 8 nm/Cheap Tubes Inc., USA	<8	2-5	10,000-30,000	500
II	Multiwalled carbon nanotubes 50 nm/Cheap Tubes Inc., USA	50-80	5-10	10,000-20,000	60
III	COOH functionalized graphitized multiwalled carbon nanotubes 20-30 nm/Cheap Tubes Inc., USA	20-30	5-10	10,000-30,000	55
IV	Carbon nanotube, single-walled/Sigma-Aldrich	2	No data	3000	>1000 (BET)
V	Carbon nanohorns, as grown/Sigma-Aldrich	2-5 (by TEM)	No data	4-5	400 (BET)
VI	Carbon nanohorns, oxidized/Sigma-Aldrich	2-5 (by TEM)	No data	4-5	1300-1400 (BET)

*SSA: specific surface area (as declared by the suppliers).

theoretical and experimental studies [17–19]. Direct contact of NPs with cellular membranes of the respiratory system is possible only after their transfer across the protective layer of lung liquids. Bronchial tree is lined by a relatively thick layer of viscous mucus which limits the penetration of NPs to the epithelial cells. In contrast, the alveolar (pulmonary) region is covered by the ultrathin aqueous film which contains the lung surfactant (LS). LS forms a monolayer at air/liquid interface, i.e., the structure which resembles a single part of biological membranes; however, dynamic conditions in which LS exists are exceptional. Breathing cycle induces the periodic extension and contraction of LS monolayer; therefore, the surfactant always remains under nonsteady-state dynamic conditions. Molecular rearrangement of LS at the air/liquid interface and possible mass exchange with the liquid sublayer result in variations of the surface concentration and surface tension. Due to an intrinsic kinetics of these processes, LS system exhibits a dynamic viscoelastic response which is manifested by a time shift between the mechanical perturbation (surface deformation) and the surface concentration/tension. These properties have physiological consequences and they also require the specific (dynamic) conditions of experimental analysis [20].

Presented study is focused on the measurements of the influence of selected CNTs/CNHs with variable surface properties on the phospholipid layer (as a functional model of biological membrane) and on the dynamic model of LS interface at simulated physiological conditions. The experiments are done with two techniques: (i) Langmuir trough and (ii) dynamic pendant drop (DPD) tensiometry. Both methods allow to evaluate the influence of tested nanomaterials on mechanical properties of interfacial films which may be linked to the mass transfer properties in biological lipid layers in vivo.

2. Materials and Methods

2.1. Materials. Ultrapure water (Puricom, USA/Millipore, Germany) was used in all studies. Dipalmitoyl phosphatidylcholine (DPPC, 99.9% pure from Sigma-Aldrich) was used as obtained to prepare the solution (1 mg/ml) in the mixed solvent of hexane : ethanol, 9 : 1 (Merck, Germany).

Survanta (Abbott Labs., France) was used as a model of multicomponent lung surfactant. The stock solution was diluted either with ultrapure water or with aqueous suspensions of NPs to obtain the final phospholipid concentration 2.5 mg/ml, which is in the range of physiological values [21].

Different types of nanotubes and nanohorns were obtained from two suppliers (Table 1). Multiwalled nanotubes were denoted as I-III, single-walled nanotubes as IV, and nanohorns as V and VI.

2.2. Experimental Techniques and Data Analysis. Carbon nanomaterials were characterized by scanning electron microscopy (SEM, Ultra Plus, Zeiss, Germany) and their SSA was measured by N_2 adsorption in Gemini 2360 apparatus (Micromeritics Instrument Corp., USA) using multipoint BET method.

As mentioned earlier, the measurements focused on particle-surface interactions were done in two experimental systems. Thermostated Langmuir trough equipped with moveable barriers and Wilhelmy balance (LB Minitrough, KSV Instruments, Finland) was used to study compression isotherms of a model phospholipid monolayer (DPPC). These isotherms, i.e., the relationships of surface pressure π vs. interfacial area A, were measured at 37°C at quasistatic conditions (rate of surface reduction: 1.25 cm^2/s). Carbon nanomaterials were applied directly on the lipid film by depositing 25 μl of the suspension of tested CNMs in hexane : ethanol, 9 : 1 (hydrophobic particles: I, II, IV, and V) or in ethanol (hydrophilic particles: III and VI). Concentrations of organic suspensions were initially adjusted to obtain the desired particle contents in the system after deposition of the sample. Each NP suspension was sonicated prior to application to disintegrate particle aggregates. Compression of the film was started 20 min after application of organic solution and CNM suspension. This time was necessary for the complete evaporation of the solvent from the air/liquid interface.

The effect of different concentrations of various carbon nanomaterials on the lipid layer may be assessed by qualitative comparison of the shape of π-A isotherm curves; however, a more articulate information on mechanical effects in the monolayer can be gathered from surface compressibility

functions. Isothermal surface compressibility κ is a reciprocal of dilatational elasticity of the interfacial region ε (sometimes also called the compressibility modulus C_s^{-1} [22]):

$$\kappa = -\frac{1}{A}\left(\frac{dA}{d\pi}\right)_T = \frac{1}{\varepsilon}. \quad (1)$$

A schematic curve of κ as a function of π is schematically shown in Figure 1 together with a sample π-A isotherm. The characteristic maximum of compressibility κ_{max} corresponds to the most horizontal part of a plateau on the isotherm in the coexistence region (LE-LC indicated by arrow in the inset of Figure 1) after which a rapid condensation of the monolayer begins. Increase in κ_{max} denotes a higher fluidity of the phospholipid layer in the coexistence region, where condensed lipid domains are floating in the expanded phase. This suggests that the monolayer in this range can be compressed to lower values of the surface pressure, which also means that the surface tension in the system cannot be reduced as much as in systems characterized by lower κ_{max}. If κ_{max} is decreased, the situation is opposite, i.e., the monolayer becomes more stiff due to a faster lipid condensation of lipid molecules.

Discussion of concentration effects of each type CNMs can be simplified and generalized by introducing a dimensionless factor $\Delta\kappa_{max}$ which indicates the relative changes of the maximum compressibility of the lipid film:

$$\Delta\kappa_{max} = \frac{\kappa_{max,c} - \kappa_{max,0}}{\kappa_{max,0}} \times 100\%, \quad (2)$$

where $\kappa_{max,c}$ is the maximum film compressibility value at CNM concentration c, and $\kappa_{max,0}$ is the maximum compressibility value of a pure phospholipid film.

The second technique used in this study—the DPD tensiometry—also allows to determine mechanical properties of air/liquid interface enriched in a surface-active material, but these data correspond to a dynamic situation. As indicated in the previous section, the multicomponent lung surfactant (Survanta) was used to produce a small pendant drop with the initial surface area of 16 mm^2. The droplet was then oscillated at 10% surface area changes with various frequencies (0.1-0.5 Hz) which correspond to a range of breathing patterns (2 s–10 s per inspiration-expiration cycle). In these experiments, particles were mixed with ultrapure water in the ultrasonic bath (Sonorex RK 108, Bandelin Electronic, Germany) and then the mixture was added to Survanta, vortexed, and thermostated for 15 minutes at 37°C. After that, the sample was used for dynamic surface tension measurements in PAT-1M device (Sinterface Technologies, Germany).

Sinusoidal oscillations of the interfacial area A result in periodic variations of the surface tension γ, with γ-A hysteresis being a common effect related to viscoelastic properties of the surfactant-rich air/liquid interface. This hysteresis in the lung surfactant system is associated with essential physiological functions. It is recognized that the unique, hysteretic variations of the surface tension in pulmonary alveoli during breathing are indispensable for the proper lung ventilation

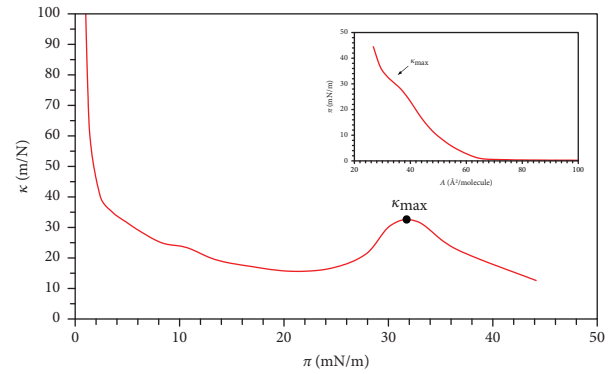

Figure 1: Surface compressibility κ as a function of surface pressure π. The inset shows the corresponding compression isotherm π (A).

but also provide a mechanism for the initiation of dynamic Marangoni effects which contribute to the intrapulmonary mass transfer (e.g., the clearance of particulate deposits, transmembrane gas exchange, and absorption of drugs) [20]. Consequently, some viscous (dissipative) effects at the deformable air/liquid interface of the lungs are essential to maintain these vital functions. On the other hand, a certain degree of surface elasticity is critical to assure the sufficient range of surface tension variations during inspiration and expiration which play an important role in breathing mechanics [23].

Two quantitative parameters may be obtained from a series of oscillatory γ-A experiments done in DPD method: dilatational surface elasticity ε and dilatational surface viscosity μ. These parameters fully characterize the mechanical response of the interfacial layer to periodic breathing-like deformations. Viscoelasticity in a periodic system may be expressed using the complex notation:

$$\varepsilon^* = \varepsilon + i\omega\mu, \quad (3)$$

where i denotes the imaginary unit and ω means the oscillation frequency. Accordingly, the loss angle φ (as the indicator of the significance of viscous-to-elastic properties) is defined as follows:

$$\varphi = arc\,tg\left(\frac{\mu\omega}{\varepsilon}\right). \quad (4)$$

The relation between the loss angle and the hysteresis is schematically shown in Figure 2, which indicates that a large hysteresis is obtained at higher φ. Therefore, the loss angle allows to identify directly the influence of the applied experimental conditions on the surface tension hysteresis in LS system.

3. Results and Discussion

Figure 3 shows SEM micrographs of all tested nanomaterials. The pictures confirm particle structure and size declared by the suppliers (Table 1). CNTs in sample IV (single-walled) are characterized by the smallest external diameter which corresponds to their large SSA. MWCNTs II and III are

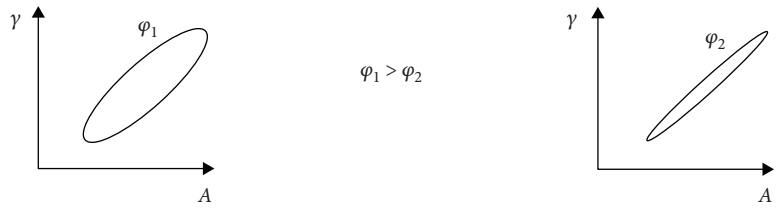

Figure 2: Schematic relationship between the loss angle φ and the surface tension hysteresis (γ-A).

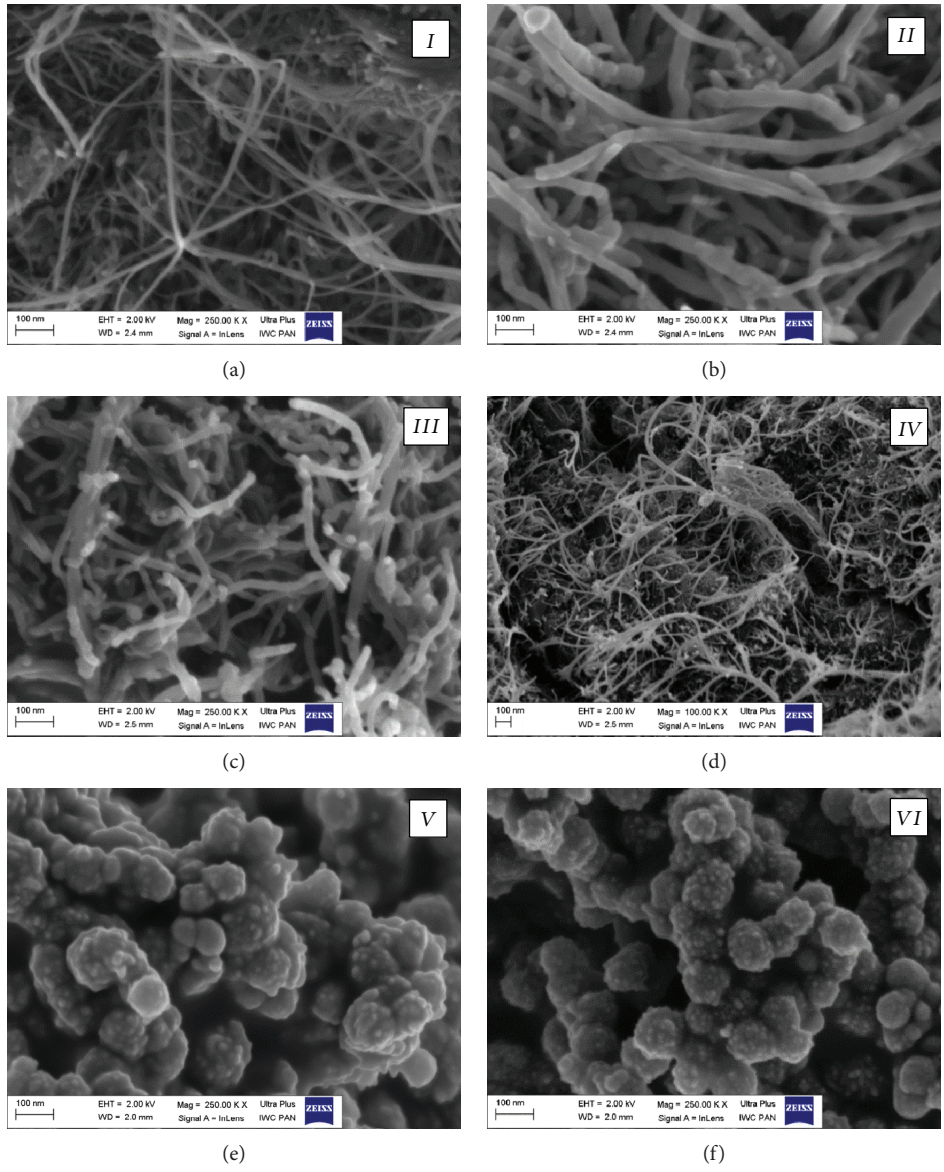

Figure 3: SEM micrographs of tested carbon nanotubes CNTs I–IV (a–d) and nanohorns CNHs V-VI (e–f). Sample designations according to Table 1.

similar in geometry (diameter, length) and declared SSA. Fibers I have a diameter between these extremes. CNHs have quite a different structure than CNTs and their length-to-diameter ratio is close to unity. It is also visible that they more easily aggregate than any CNTs and that they form larger fractal-like structures. Interestingly, two types of CNHs differ significantly in the declared (and the measured—see Table 2) specific surface area. This may be explained by a more corrugated surface of particles VI due to chemical functionalization (oxidation) but also by a less tendency to aggregate as compared to particles V (single separate NPs can be detected in Figure 3(f)).

The results of SSA data obtained in our studies are listed in Table 2 and they show that sporadically declared data

Table 2: Specific surface area of tested carbon nanomaterials: measured in this study SSA_{exp} and declared by the suppliers SSA_{dec}.

CNM designation	I	II	III	IV	V	VI
SSA_{exp} (m^2/g)	445 ± 10	92 ± 2	190 ± 4	935 ± 20	396 ± 10	1279 ± 28
SSA_{dec} (m^2/g)	500	60	55	>1000	400	1300-1400

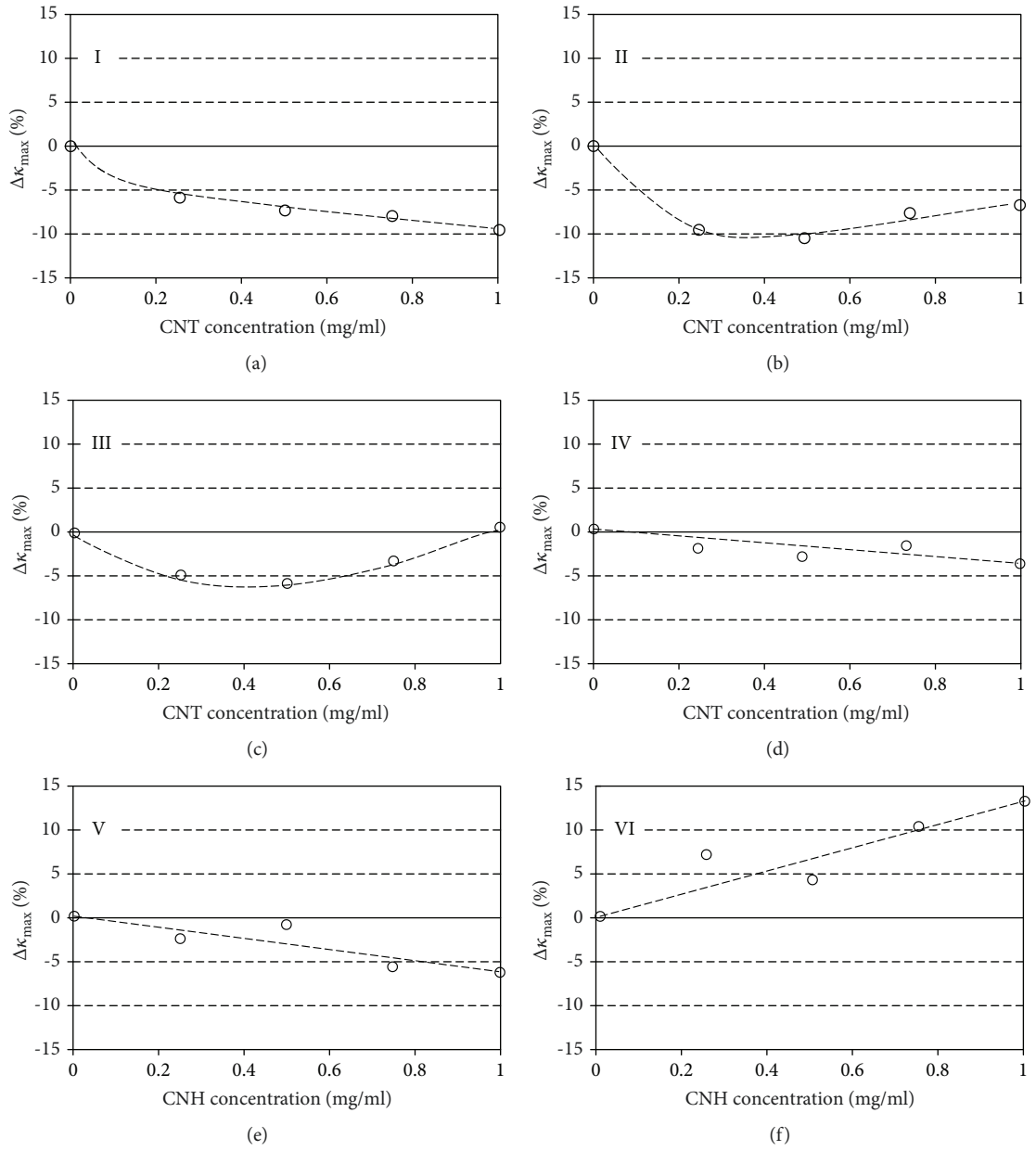

Figure 4: The relative deviation of the maximum surface compressibility for DPPC monolayer after contact with different CNTs and CNHs. Dashed lines are drawn to guide the eye.

deviate from experimental results obtained for the samples (e.g., functionalized MWCNTs III).

Figure 4 depicts changes of $\Delta\kappa_{max}$ after contact of studied CNMs with biomimetic phospholipid layer during quasi-static Langmuir trough experiments. The results show that particle wettability and SSA are the main determinants of interactions with the biomimetic membrane. It can be easily explained by the fact that interactions at the air/liquid interface require a direct contact between lipid molecules and NPs which actually leads to reorientation and bonding of lipid molecules to the surface of nanomaterials (i.e., adsorption) [24].

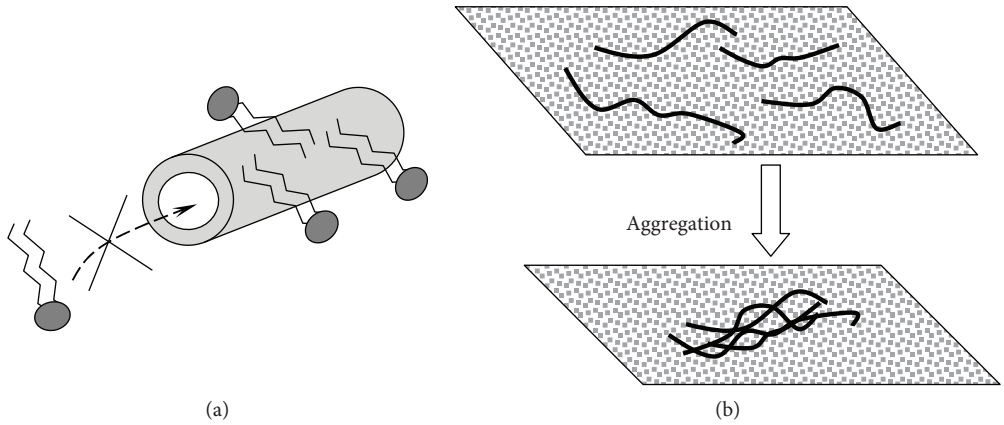

Figure 5: (a) Schematic illustration of DPPC adsorption on the external surface of hydrophobic CNTs and a restricted accessibility of phospholipids to the CNTs interior. (b) Explanation of the influence of CNT aggregation on the reduction of their area of interactions with DPPC at the air/liquid interface.

The association between the total SSA measured by nitrogen sorption and the degree of CNMs-DPPC interactions may be reduced due to the limited access of relatively large phospholipid molecules to the internal surface of CNMs (Figure 5(a)). It is observable in case of SWCNTs IV with a small external diameter which promote a low effect regarding $\Delta\kappa_{max}$ in spite of their large SSA_{exp} (Figure 4(d)). Hydrophobic CNMs I, II, IV, and V decrease the maximum compressibility (i.e., increase the maximum surface elasticity), most probably due to mutual interactions with the hydrocarbon chains of phospholipids on the air/liquid interface. The observed effects are concentration-dependent, and—in general—they are increased at higher NP contents. A difference is found only for particles II, where a minimum of $\Delta\kappa_{max}$ at moderate concentration (0.25-0.5 mg/ml) is observed and followed by a partial recovery of this parameter when CNT concentration approaches 1 mg/ml. Such effect is probably associated with a relatively low SSA of these MWCNTs (~90 m^2/g) which can be additionally reduced when nanotubes are more aggregated due to increased concentration (Figure 5(b)). In this situation, a reduced contact and weaker interactions take place between CNTs and phospholipid molecules.

In contrast to hydrophobic CNTs, functionalized (oxidized) nanohorns VI—which are characterized by the highest SSA among all tested nanomaterials (Table 2)—cause a concentration-dependent increase in $\Delta\kappa_{max}$ (up to 15% at 1 mg/ml). It is an effect of high surface area of these particles rather than of their hydrophilicity. It may be confirmed by the observation that carboxylated MWCNTs with low SSA (~190 m^2/g—sample III) induce a comparable effect as hydrophobic particles with similarly low specific surface area (sample II).

Analysis of CNTs-CNHs interactions with the lung surfactant model in dynamic conditions is done in Figure 6 which shows variations of surface dilatational elasticity ε and viscosity μ as a function of CNM concentration. These data are obtained at fixed oscillation frequency 0.25 Hz which corresponds to the typical breathing rate at rest (4 s per inhalation and exhalation cycle).

In all cases, the elasticity increases in a dose-dependent manner when CNMs are present in the system. The maximum elasticity of 130 mN/m is observed for hydrophobic CNTs with high SSA (IV) at the maximum concentration (1 mg/ml). Interestingly, hydrophilic CNHs with high SSA (VI) cause less significant changes in the surface elasticity but they decrease the viscosity. Some changes in the elasticity are also observed for hydrophobic CNMs with a low and medium SSA (e.g., I, II, and V). These particles almost do not change the dissipative properties of the surface (i.e., the dilatational surface viscosity). For particles I, IV, and V, the surface elasticity of air/liquid interface gradually increases with the increasing concentration. It may be noticed that these results correlate with a gradual drop of the maximum surface compressibility $\Delta\kappa_{max}$ observed for the same particles in the Langmuir trough during experiments with DPPC monolayer. A strong increase in ε for CNTs IV is probably due to their high SSA which promotes more powerful hydrophobic cohesive interactions with surfactant molecules. A different effect of surface elasticity for LS contacted with CNMs has been found for CNTs II where the maximum ε value at moderate particle concentration is followed by a decrease of the elasticity at the highest CNTs content. Again, this observation corresponds to the abnormal dependence of $\Delta\kappa_{max}$ found in the monolayer studies (Figure 4(b)) and may be linked to a reduction of contact area due to CNT aggregation (Figure 5(b)).

In contrast to hydrophobic CNMs, hydrophilic CNTs III and CNHs VI cause a very small increase of the surface elasticity, and the highest concentration of CNHs VI results in the return of ε to the initial (control) value (Figure 6(f)). As indicated earlier, only for these two types of hydrophilic CNMs a concentration-dependent drop in surface viscosity can be observed. This suggests that LS interface becomes less dissipative (i.e., more reversible) during breathing-like oscillations when hydrophilic particles are present in the system. It may have certain physiological consequences in vivo since—as already mentioned—the native viscoelastic properties of the air/liquid interface of the alveolar region are closely related to the surface tension hysteresis as the important and

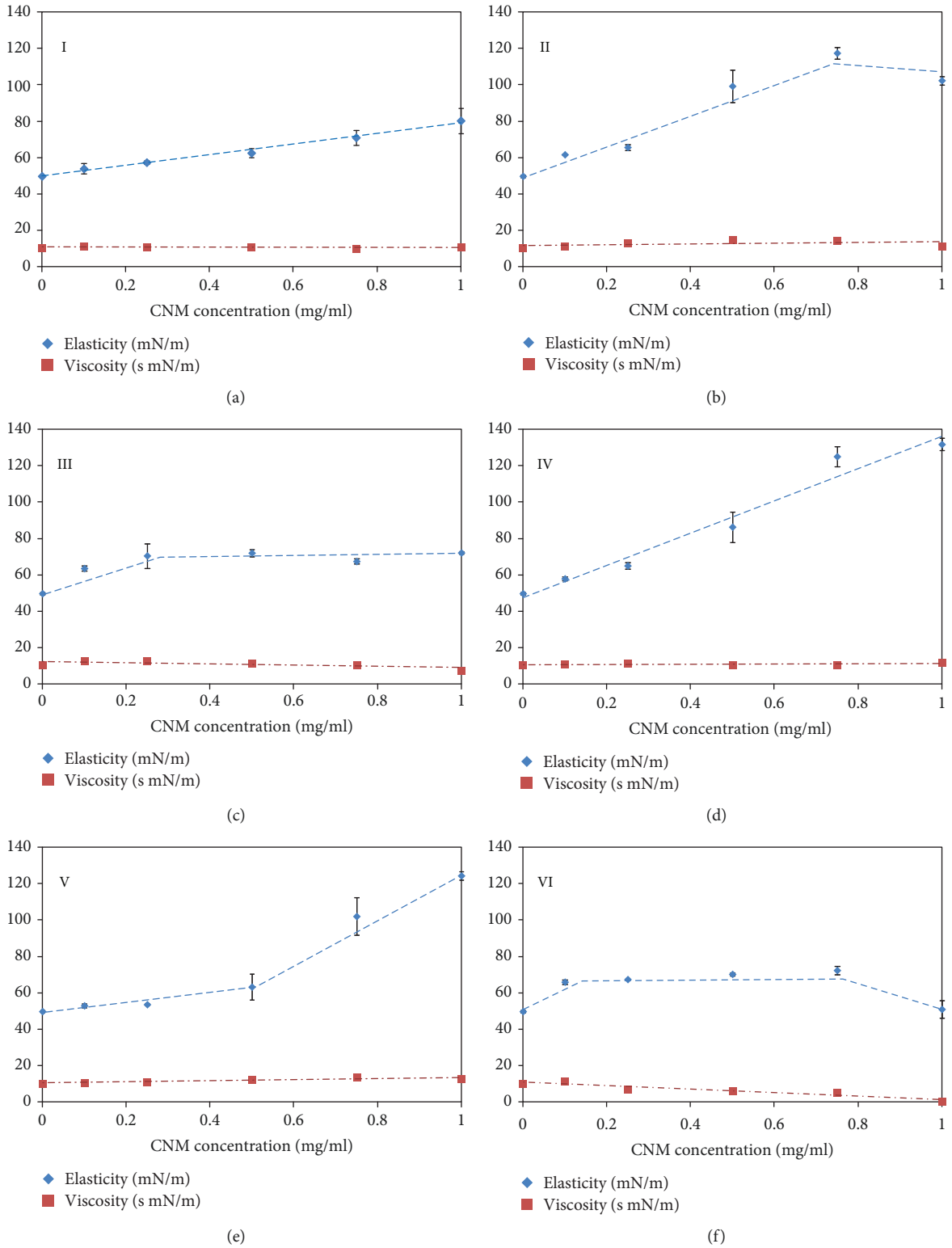

FIGURE 6: Surface dilatational elasticity and viscosity of oscillated air/liquid interface of LS contacted with tested CNMs at different concentration (oscillation frequency 0.25 Hz, $T = 37^{\circ}$C). Dashed lines are drawn to guide the eye.

characteristic feature of the lung surfactant. The γ-A hysteresis reflects the ability of the lung surfactant to modulate the surface tension of the alveolar liquid during breathing cycle in a way which leads to generation of the Marangoni effects as important mechanism of the alveolar hydrodynamics and mass transfer [20, 25]. Consequently, a reduction of measured γ-A hysteresis, as a result of decreased viscosity of the interfacial region, will cause a deviation from the

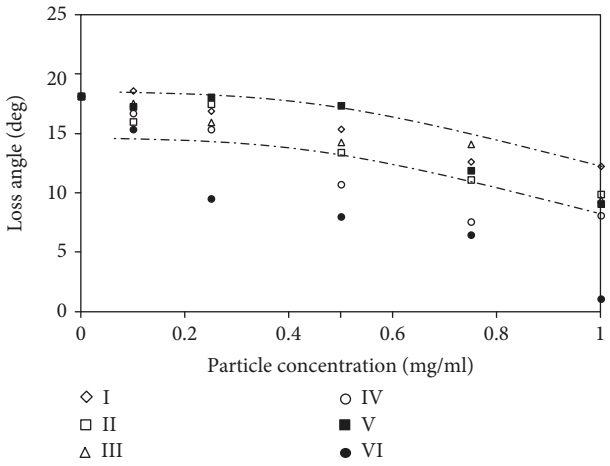

Figure 7: Change in the loss angle φ after LS contact with tested CNTs and CNHs (surface oscillation rate: 0.25 Hz, $T = 37^{\circ}$C).

normal functionality of the LS [26, 27]. Figure 7 shows how the loss angle (as a measure of the hysteresis, Figure 2) is changed at different concentrations of studied CNTs and CNHs. All but two types of CNMs reduce the loss angle in a similar dose-dependent manner—all φ values lie in the region between two dashed lines drawn in Figure 7. Two types of CNMs (IV and VI) cause a noticeably stronger effect and reduce the loss angle to less than 10 deg. These particles differ in wettability (IV are hydrophobic; VI are hydrophilic); however, both are characterized by very large SSA (900-1300 m^2/g). It is therefore plausible that SSA rather than surface hydrophobicity or hydrophilicity are more important determinants of the influence of nanoparticles on the surface tension hysteresis under dynamic breathing-like conditions.

Presented data allow to state that interactions of studied CNMs with model phospholipid monolayer under quasistatic conditions and interactions of these CNMs with multicomponent model of the lung surfactant under breathing-like conditions deliver different information regarding the influence of particle surface (size, geometry, SSA, and wettability) on lipid layers. For DPPC in studied in Langmuir trough, particle wettability plays the most important role by allowing NPs to interact with phospholipid molecules present at the air/liquid interface. It may be an important issue if functionalized (hydrophilic) CNMs are introduced into the organism, e.g., as drug carriers. According to the results of several different studies, hydrophilic NPs form partially hydrophobic complexes with lipids and this results in alteration in molecular arrangement and surface mechanical properties in the LE-LC coexistence region of the interfacial layer [28–30]. Increase in surface compressibility κ suggests the reorientation/rearrangement of LC domains during monolayer compression but also a partial removal of these complexes from the interface (monolayer refinement [20]). Such effect was also demonstrated by MD simulations [31]. Larger film compressibility of the lipid film may also contribute to a wider hysteresis in periodic compression-expansion of the interfacial layer. In contrast, hydrophobic particles are known to incorporate into the lipid film and aggregate at LC domain boundaries. This modifies cohesive interactions in the monolayer and results in delayed film condensation and a steeper isotherm in the coexistence region [32]. As a consequence, the maximum surface compressibility κ_{max} should be reduced which was confirmed by our results for hydrophobic CNTs and CNHs (Figure 4). It has been also speculated that removal of hydrophobic NPs from the monolayer upon high compression (i.e., condensed film at high surface pressure) causes also a transfer of considerable amounts of adsorbed lipid molecules [30, 31] which agrees with the proposed conception of lipid adsorption to the surface of hydrophobic CNTs (Figure 5(a)). Differences in the effects caused by hydrophilic and hydrophobic CNMs observed in this study are also in accord with the previous data obtained for other materials with variable wettability [24].

For dynamic surface deformations where interfacial processes run in a short time scale, the effects of CNTs/CNHs surface wettability appeared to be also important (Figure 6). However, the hysteretic response of the surface tension to the breathing-like periodic deformations of air/liquid interface in the model LS system was also quite sensitive to the surface area of CNMs. The loss angle which characterizes the viscous part of the mechanical response of the interface and influences the width of the γ-A hysteresis is reduced stronger by CNMs with high SSA, independently of their wettability. Such conclusion agrees with a recognized positive correlation between the health effects in the lungs and the total surface area of inhaled NPs (rather than the total inhaled mass) [33]. Less important role of NP wettability may be explained here by the fact that LS (and DPPC) molecules are amphiphilic, so they can be adsorbed on both types of solid surface. Another important issue is aggregation or dispersion of CNMs during the contact with the constituents of the interfacial layer (this problem was discussed, e.g., in [34]). Our results suggest that CNM aggregation at the interface may partially restrict the area of NPs-lipid interactions; therefore, they reduce the surface effects.

4. Conclusions

Presented studies analyzed direct physicochemical interactions between selected carbon nanomaterials (CNTs and CNHs with various surface properties) with biomimetic lipid layers under quasistatic and dynamic conditions. It was confirmed that the effective (available) surface area of nanoparticles and their wettability are the main determinants of these highly specific interactions; however, both parameters have a different impact on mono- and multicomponent lipid layers under quasistatic or dynamic conditions. In particular, the viscoelastic properties of the dynamic lung surfactant layer which are essential for LS physiological functions and pulmonary mass transfer [20, 23, 25] can be significantly changed by CNTs and CNHs with a high surface area (~1000 m^2/g). This confirms that NP surface rather than mass is the decisive factor and the proper metrics in the assessment of health effects from inhaled carbon nanomaterials.

Abbreviations

A: Surface area
C_s^{-1}: Surface compressibility modulus
i: Imaginary unit
T: Temperature
γ: Surface tension
ε: Dilatational surface elasticity
φ: Loss angle
κ: Surface (film) compressibility
$\Delta\kappa_{max}$: Relative change of the maximum surface compressibility
μ: Dilatational surface viscosity
π: Surface pressure
ω: Oscillation frequency
CNH: Carbon nanohorn
CNM: Carbon nanomaterial
CNT: Carbon nanotube
DPD: Dynamic pendant drop
DPPC: 1,2-Dipalmitoyl-3-phosphatidylcholine (1,2-dipalmitoyl glycero-3-phosphocholine)
LC: Liquid-condensed phase
LE: Liquid-expanded phase
LS: Lung surfactant
MD: Molecular dynamics
MWCNT: Multiwalled carbon nanotube
NP: Nanoparticle
SEM: Scanning electron microscopy
SSA: Specific surface area
SWCNT: Single-walled carbon nanotube.

Data Availability

The data used to support the findings of this study are included within the article.

Conflicts of Interest

The authors declare that there is no conflict of interests regarding the publication of this paper.

Acknowledgments

This paper has been based on the results of a research task no. II.N.10 carried out within the scope of the fourth stage of the national program "Improvement of safety and working conditions" partly supported in 2017–2019—within the scope of research and development—by the Ministry of Science and Higher Education/National Centre for Research and Development. The Central Institute for Labour Protection-National Research Institute is the program's main coordinator. Theoretical analysis developed by TRS was supported by the NCN project no. 2014/13/B/ST8/00808.

References

[1] P. H. M. Hoet, I. Brüske-Hohlfeld, and O. V. Salata, "Nanoparticles – known and unknown health risks," *Journal of Nanobiotechnology*, vol. 2, no. 1, p. 12, 2004.

[2] W. Yang, J. I. Peters, and R. O. Williams III, "Inhaled nanoparticles—a current review," *International Journal of Pharmaceutics*, vol. 356, no. 1-2, pp. 239–247, 2008.

[3] Research and Markets, "Global carbon nanotubes market - by type, application, method, end-use, the region - market size, demand forecasts, industry trends and updates (2016–2022)," 2017, May 2017, https://www.researchandmarkets.com/reports/4401828.

[4] J. Kayat, V. Gajbhiye, R. K. Tekade, and N. K. Jain, "Pulmonary toxicity of carbon nanotubes: a systematic report," *Nanomedicine: Nanotechnology, Biology and Medicine*, vol. 7, no. 1, pp. 40–49, 2011.

[5] V. Castranova, P. A. Schulte, and R. D. Zumwalde, "Occupational nanosafety considerations for carbon nanotubes and carbon nanofibers," *Accounts of Chemical Research*, vol. 46, no. 3, pp. 642–649, 2013.

[6] R. R. Mercer, J. F. Scabilloni, A. F. Hubbs et al., "Distribution and fibrotic response following inhalation exposure to multiwalled carbon nanotubes," *Particle and Fibre Toxicology*, vol. 10, no. 1, p. 33, 2013.

[7] J. H. Han, E. J. Lee, J. H. Lee et al., "Monitoring multiwalled carbon nanotube exposure in carbon nanotube research facility," *Inhalation Toxicology*, vol. 20, no. 8, pp. 741–749, 2008.

[8] N. Karousis, I. Suarez-Martinez, C. P. Ewels, and N. Tagmatarchis, "Structure, properties, functionalization, and applications of carbon nanohorns," *Chemical Reviews*, vol. 116, no. 8, pp. 4850–4883, 2016.

[9] Y. Yang, Z. Qin, W. Zeng et al., "Toxicity assessment of nanoparticles in various systems and organs," *Nanotechnology Reviews*, vol. 6, no. 3, pp. 279–289, 2017.

[10] S. Tatur and A. Badia, "Influence of hydrophobic alkylated gold nanoparticles on the phase behavior of monolayers of DPPC and clinical lung surfactant," *Langmuir*, vol. 28, no. 1, pp. 628–639, 2012.

[11] M. Geiser and W. G. Kreyling, "Deposition and biokinetics of inhaled nanoparticles," *Particle and Fibre Toxicology*, vol. 7, no. 1, p. 2, 2010.

[12] O. Creutzenberg, "Biological interactions and toxicity of nanomaterials in the respiratory tract and various approaches of aerosol generation for toxicity testing," *Archives of Toxicology*, vol. 86, no. 7, pp. 1117–1122, 2012.

[13] C. Von Garnier, B. Rothen-Rutishauser, and F. Blank, "Nanoparticles in the respiratory tract: modulation of antigen-presenting cell function," *Journal of Environmental Immunology and Toxicology*, vol. 1, no. 3, pp. 140–149, 2013.

[14] G. Oberdörster, A. Elder, and A. Rinderknecht, "Nanoparticles and the brain: cause for concern?," *Journal of Nanoscience and Nanotechnology*, vol. 9, no. 8, pp. 4996–5007, 2009.

[15] M. I. Sajid, U. Jamshaid, T. Jamshaid, N. Zafar, H. Fessi, and A. Elaissari, "Carbon nanotubes from synthesis to in vivo biomedical applications," *International Journal of Pharmaceutics*, vol. 501, no. 1-2, pp. 278–299, 2016.

[16] S. A. Chechetka, M. Zhang, M. Yudasaka, and E. Miyako, "Physicochemically functionalized carbon nanohorns for multi-dimensional cancer elimination," *Carbon*, vol. 97, pp. 45–53, 2016.

[17] G. Weidemann and D. Vollhardt, "Long range tilt orientational order in phospholipid monolayers: a comparison of the order in the condensed phases of dimyristoylphosphatidylethanolamine and dipalmitoylphosphatidylcholine," *Colloids*

and Surfaces A: Physicochemical and Engineering Aspects, vol. 100, pp. 187–202, 1995.

[18] Y. Li, X. Chen, and N. Gu, "Computational investigation of interaction between nanoparticles and membranes: hydrophobic/hydrophilic effect," *The Journal of Physical Chemistry B*, vol. 112, no. 51, pp. 16647–16653, 2008.

[19] T. R. Sosnowski, M. Koliński, and L. Gradoń, "Alteration of surface properties of dipalmitoyl phosphatidylcholine by benzo[a]pyrene: a model of pulmonary effects of diesel exhaust inhalation," *Journal of Biomedical Nanotechnology*, vol. 8, no. 5, pp. 818–825, 2012.

[20] T. R. Sosnowski, "Particles on the lung surface – physicochemical and hydrodynamic effects," *Current Opinion in Colloid & Interface Science*, vol. 36, pp. 1–9, 2018.

[21] E. P. Ingenito, L. Mark, J. Morris, F. F. Espinosa, R. D. Kamm, and M. Johnson, "Biophysical characterization and modeling of lung surfactant components," *Journal of Applied Physiology*, vol. 86, no. 5, pp. 1702–1714, 1999.

[22] H. Zhu, R. Sun, T. Zhang et al., "Interfacial interactions and nanostructure changes in DPPG/HD monolayer at the air/water interface," *Journal of Nanomaterials*, vol. 2015, Article ID 908585, 10 pages, 2015.

[23] J. Goerke, "Surfactant and lung mechanics," in *Pulmonary Surfactant: from Molecular Biology to Clinical Practice*, B. Robertson, L. M. G. Golde, and J. J. Batenburg, Eds., pp. 165–192, Elsevier, Amsterdam, 1992.

[24] D. Kondej and T. R. Sosnowski, "Effect of clay nanoparticles on model lung surfactant: a potential marker of hazard from nanoaerosol inhalation," *Environmental Science and Pollution Research*, vol. 23, no. 5, pp. 4660–4669, 2016.

[25] L. Gradoń and A. Podgórski, "Hydrodynamical model of pulmonary clearance," *Chemical Engineering Science*, vol. 44, no. 3, pp. 741–749, 1989.

[26] T. R. Sosnowski, "Influence of insoluble aerosol deposits on the surface activity of the pulmonary surfactant: a possible mechanism of alveolar clearance retardation?," *Aerosol Science and Technology*, vol. 32, no. 1, pp. 52–60, 2000.

[27] D. Kondej and T. R. Sosnowski, "Alteration of biophysical activity of pulmonary surfactant by aluminosilicate nanoparticles," *Inhalation Toxicology*, vol. 25, no. 2, pp. 77–83, 2013.

[28] E. Guzmán, L. Liggieri, E. Santini, M. Ferrari, and F. Ravera, "Effect of hydrophilic and hydrophobic nanoparticles on the surface pressure response of DPPC monolayers," *The Journal of Physical Chemistry C*, vol. 115, no. 44, pp. 21715–21722, 2011.

[29] E. Guzmán, E. Santini, M. Ferrari, L. Liggieri, and F. Ravera, "Effect of the incorporation of nanosized titanium dioxide on the interfacial properties of 1,2-dipalmitoyl-sn-glycerol-3-phosphocholine langmuir monolayers," *Langmuir*, vol. 33, no. 40, pp. 10715–10725, 2017.

[30] R. K. Harishchandra, M. Saleem, and H. J. Galla, "Nanoparticle interaction with model lung surfactant monolayers," *Journal of the Royal Society Interface*, vol. 7, Supplement_1, pp. S15–S26, 2010.

[31] G. Hu, B. Jiao, X. Shi, R. P. Valle, Q. Fan, and Y. Y. Zuo, "Physicochemical properties of nanoparticles regulate translocation across pulmonary surfactant monolayer and formation of lipoprotein corona," *ACS Nano*, vol. 7, no. 12, pp. 10525–10533, 2013.

[32] D. Q. Arick, Y. H. Choi, H. C. Kim, and Y. Y. Won, "Effects of nanoparticles on the mechanical functioning of the lung," *Advances in Colloid and Interface Science*, vol. 225, pp. 218–228, 2015.

[33] O. Schmid and T. Stoeger, "Surface area is the biologically most effective dose metric for acute nanoparticle toxicity in the lung," *Journal of Aerosol Science*, vol. 99, pp. 133–143, 2016.

[34] N. Nisoh, M. Karttunen, L. Monticelli, and J. Wong-ekkabut, "Lipid monolayer disruption caused by aggregated carbon nanoparticles," *RSC Advances*, vol. 5, no. 15, pp. 11676–11685, 2015.